ISSN (Print) 1226-1750
ISSN (Online) 2233-6656
Journal of Magnetics 17(4), 245-250 (2012) http://dx.doi.org/10.4283/JMAG.2012.17.4.245

Ferromagnetic Resonance and X-Ray Reflectivity Studies of Pulsed DC Magnetron Sputtered NiFe/IrMn/CoFe Exchange Bias

Ramis Mustafa Öksüzoğlu[1]*, Özlem Akman[2,3], Mustafa Yıldırım[1], and Bekir Aktaş[2]

[1]*Department of Materials Science and Engineering, University of Anadolu, 26470 Eskisehir, Turkey*
[2]*Gebze Institute of Technology, P.B. 141, 41400 Gebze-Kocaeli, Turkey*
[3]*Department of Physics, Sakarya University, 54187, Adapazarı, Turkey*

(Received 23 May 2012, Received in final form 5 September 2012, Accepted 7 September 2012)

Ferromagnetic resonance and X-ray specular reflectivity measurements were performed on $Ni_{81}Fe_{19}/Ir_{20}Mn_{80}/Co_{90}Fe_{10}$ exchange bias trilayers, which were grown using the pulsed-DC magnetron sputtering technique on Si(100)/SiO_2(1000 nm) substrates, to investigate the evolution of the interface roughness and exchange bias and their dependence on the NiFe layer thickness. The interface roughness values of the samples decrease with increasing NiFe thickness. The in-plane ferromagnetic resonance measurements indicate that the exchange bias field and the peak-to-peak line widths of the resonance curves are inversely proportional to the NiFe thickness. Furthermore, both the exchange bias field and the interface roughness show almost the same dependence on the NiFe layer thickness. The out-of plane angular dependent measurements indicate that the exchange bias arises predominantly from a variation of exchange anisotropy due to changes in interfacial structure. The correlation between the exchange bias and the interface roughness is discussed.

Keywords : ferromagnetic resonance, exchange bias, interface roughness, pulsed DC magnetron sputtering

1. Introduction

The exchange bias (EB) interaction between ferromagnetic (F) and antiferromagnetic (AF) layers [1] has attracted a lot of attention because of its importance in fundamental research and spintronic applications [2-5]. The underlying mechanism and the role of the interface/bulk structure have been investigated in a variety of EB systems [4-12] with different deposition techniques and F/AF materials. However, due to the wide variety of materials and deposition techniques used, the dependence of the EB field (H_{ex}) on the roughness is still controversial. For several systems, the H_{ex} seems to be relatively insensitive to the roughness value [7, 11], while in others the H_{ex} varies in direct proportion to the roughness [9, 10] or indicates an opposite variation [8]. Research has also shown that the relationship between the H_{ex} and the roughness value is totally different for differently prepared samples [12].

Investigations in our previous study, using a static magnetic characterization technique (superconductiong quantum interference device, SQUID), show no clear evidence for contributions from the interfacial structure and these results gave rise to the conclusion that a detailed study of the interface structure (i.e. interface roughness) is necessary to be able to discuss the influence of interface roughness on the exchange coupling properties [6]. In comparison to static magnetic measurement techniques, such as the vibration sample magnetometer (VSM) and SQUID, ferromagnetic resonance (FMR) is more sensitive to intrinsic properties down to a monolayer [13, 14] and, as such, represents a powerful tool for the determination of magnetic anisotropy of an F layer and/or an exchange coupled F/AF EB system [15]. Furthermore, the X-ray reflectivity (XRR) is a non-destructive and suitable metrology technique to precisely determine the thickness, surface and interface roughness of both transparent, metallic thin films and multilayers [16-18]. In the present study, we performed FMR and XRR studies in order to study the correlation between the exchange bias field and interface roughness.

*Corresponding author: Tel: +90-222-321-35-50
Fax: +90-222-323-95-01, e-mail: rmoksuzoglu@anadolu.edu.tr

2. Experimental

The investigated Ta(5 nm)/$Ni_{81}Fe_{19}$(*t* nm)/$Ir_{20}Mn_{80}$(10 nm) /$Co_{90}Fe_{10}$(2 nm)/Ta(5 nm) (*t* = 2-10 nm) exchange bias systems were grown on Si/SiO_2(1000 nm) substrates using the pulsed DC magnetron sputtering technique with an Ar gas pressure of 2 mTorr at room temperature. The base pressure prior to the deposition was of the order of 2×10^{-9} Torr. A pulsed DC power source (Advanced Energy, Pinnacle Plus+) was used to control the current (~10 - 11 mA) and the voltage (~350 V) supplied to the target materials (99.95% Kurt J. Lesker). The pulse was operated at a frequency of 50 kHz and had a width of 5 μs for all layers. The substrate to source angle was 68° (measured from the surface normal of the substrate) with substrate rotation of 60 rpm. An *in situ*, in-plane magnetic field of 0.5 kOe was applied during the growth. The so-called unidirectional post-annealing was performed after deposition at 200ºC for 1 hour without breaking the vacuum ($\leq 5 \times 10^{-7}$ Torr) and then the samples were field-cooled to room temperature in the same magnetic field as applied during the deposition. Each set of specimens was grown during the same vacuum cycle. The thicknesses of the layers were determined using the XRR technique. The *ex-situ* XRR measurements were carried out using a Bruker 4-circle diffractometer equipped with a Cu sealed tube point source and a Göbel Mirror optic to generate a 2D-collimated parallel beam (divergence ca. 0.03°, a lateral length 18 mm and wavelength $\lambda = 0.15406$ nm). The experimental specular XRR data was analyzed using commercial Diffrac Plus LEPTOS software. Using a genetic algorithm, the best-fit simulations to the experimental data were carried out for the EB structures by automatically adjusting the following parameters: layer thicknesses, root mean square roughness values and mass densities. Since the diffuse scattering contribution is negligible (2 cps compared to measured incident intensity of 1.5×10^7 cps), it was not subtracted from the measured specular reflectivity.

X-Ray Diffraction (XRD) and Rocking Curve (RC) measurements were carried out in order to investigate the evolution of the grain size and texture. The RC patterns were collected by fixing the 2Θ angle to the IrMn(111) diffraction peaks, which were measured by XRD Θ-2Θ scans. The full width at half maximum (FWHM) of the RCs gives information about the alignment of the grains in the IrMn(111) film plane. The FWHM is reduced when the alignment (i.e. texture) improves.

The field derivative FMR absorption spectra were recorded using a Bruker EMX type Electron Paramagnetic Resonance (EPR) spectrometer in the X-band frequency (9.5~9.8 GHz) at room temperature. The NiFe thickness dependence of the EPR spectra was investigated for both in-plane and out-of-plane geometries. In the in-plane geometry, a DC external magnetic field was applied to the surface of the films, and in the out-of-plane geometry the external magnetic field was continuously rotated in the y/z out of plane direction given by the angle θ_H, which is measured with respect to the z-axis.

3. Results and Discussion

In order to study the evolution of the individual functional film thicknesses and the interface roughness values with the thickness variation of the NiFe layer, a detailed XRR study was performed for all samples. Fig. 1 shows the experimental XRR data and their corresponding best-fit curves. The individual thickness and roughness values obtained from the best-fit simulations to the experimental data are summarized in Table 1 (the error factor amounts ~%2.5). The fit results indicate that all samples show growth of a top tantalum oxide (~2.5 nm thick) at the expense of the metallic Ta capping layer, as would be expected for a highly reactive metal after post-heat treatment. The thickness values of the individual layers in the EB samples are consistent with the deposition values including the interface roughness and the error factor. As can be seen in Table 1, for low NiFe thicknesses, the interface roughness values are relatively high, especially at the NiFe/IrMn interface, these values decrease with increasing NiFe layer thickness. In the XRR spectrum of the multilayer with a NiFe thickness equal to 10 nm (Fig.

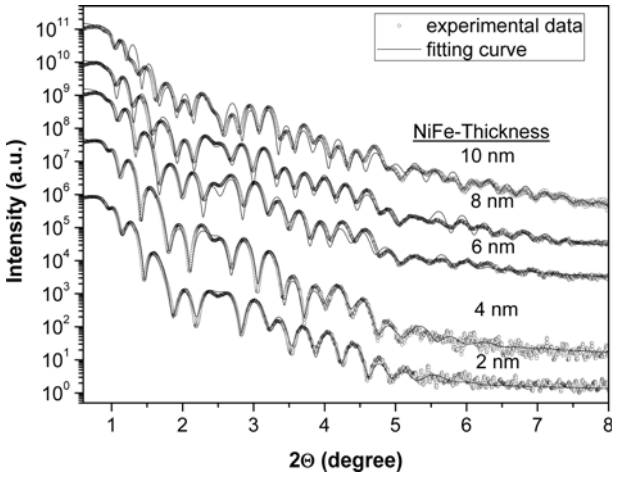

Fig. 1. The experimental XRR data (open circles) and the corresponding best fit simulations (straight lines) of the Ta(5 nm)/$Ni_{81}Fe_{19}$(*t* nm)/Ir20Mn80(10 nm)/Ta(5 nm) samples for different NiFe thicknesses (*t* = 2-10 nm). The curves are vertically shifted for clarity.

Table 1. Individual layer thicknesses t (nm) and interface roughness σ (nm) values of the samples obtained from the best fits to the experimental XRR data.

NiFe thickness	2 nm		4 nm		6 nm		8 nm		10 nm	
	t (nm)	σ (nm)	t (nm)	σ (nm)	t (nm)	σ (nm)	t (nm)	σ (nm)	t (nm)	σ (nm)
Ta_2O_5	2.50	0.60	2.57	0.71	2.72	0.52	2.65	0.44	2.52	0.58
Ta (5 nm)	4.50	0.61	4.55	0.69	4.18	0.52	4.20	0.46	4.62	0.52
CoFe (2 nm)	1.65	0.62	1.70	0.59	1.74	0.50	1.74	0.50	1.75	0.50
IrMn (10 nm)	10.20	0.64	9.51	0.50	9.95	0.42	10.4	0.40	9.75	0.39
NiFe (t_s = 2-10 nm)	**1.40**	**0.72**	**3.36**	**0.57**	**5.32**	**0.52**	**7.44**	**0.46**	**10.70**	**0.43**
Ta (5 nm)	5.48	0.54	5.34	0.55	5.15	0.53	5.54	0.53	5.30	0.50

1), the differences between the measured and calculated spectrum, especially in the central part of the spectrum, can be explained as follows: Due to the low CoFe layer thickness (< 2 nm), the layer parameters as the layer thickness and, especially, interface roughness and density influence the main part of the spectrum and cannot be well estimated. The layer thickness and roughness of the top Ta-Oxide, Ta, IrMn and NiFe layers can be well estimated, however; the parameters of the bottom Ta layer are not easily found. This is attributable to the reducing resolution with increasing absorption in the sample when the NiFe thickness is equal to 10 nm. The specular total reflection of this sample is reduced (~1.5×10^7 cps) in comparison to the remaining multilayers with lower NiFe thicknesses (~7×10^6 cps) indicating an enhancement of the absorption and consequently a reduction of the resolution, especially for low layer thicknesses.

In order to clarify, the effect of the grain size and texture, XRD and RC measurements were carried out (not given here). The average grain size of the AF IrMn layer was calculated from the FWHM of the IrMn(111) peak by using Scherrer's equation. Figure 2 shows the grain size in the IrMn layer and the FWHM of the RCs and their dependence on the thickness of the NiFe layer. As can be seen in Fig. 2, the FWHM values and the average grain size in the IrMn layer do not vary within the error factor, which reveal that the <111> out-of plane texture and grain size are not affected significantly by the thickness of the NiFe layer. Accordingly, the observed roughness effects in the investigated samples can be isolated from the grain size and the texture.

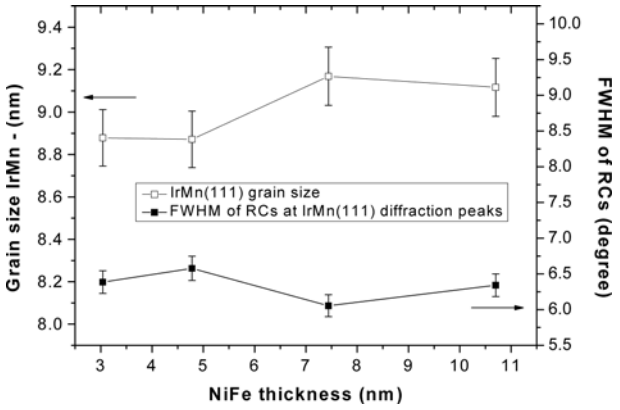

Fig. 2. Grain size in the IrMn layer and FWHM of the RCs of the IrMn(111) diffraction peaks and their dependence on the thickness of the NiFe layer.

In order to determine the evolution of H_{ex}'s dependence on the NiFe layer thickness, FMR measurements were carried out. The advantage of angular dependent FMR measurements compared with VSM is, in addition to dc magnetization, magnetic anisotropy parameters, any g value and exchange parameter can be determined. Furthermore, FMR is very sensitive; it sense of internal field and its accuracy does not depend on the amount of the sample

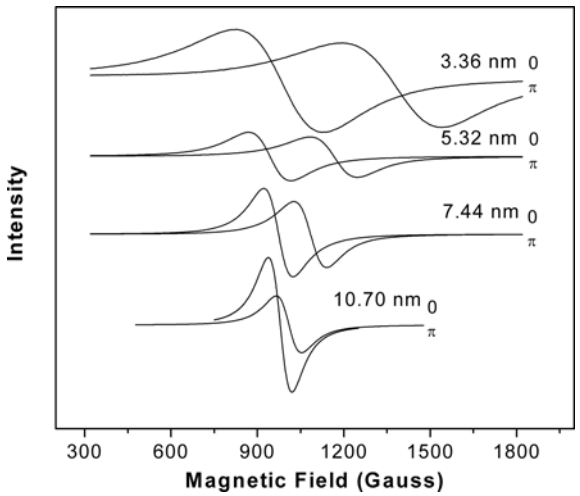

Fig. 3. The room temperature FMR spectra of the $Ni_{81}Fe_{19}$/$Ir_{20}Mn_{80}$/$Co_{90}Fe_{10}$ trilayer system with in-plane geometry for the external field parallel (0) and antiparallel (π) to the exchange anisotropy direction for different NiFe layer thicknesses, which were obtained from the XRR study (Fig. 1 and Table 1). The resonance spectra arise from the NiFe layers (see text). The resonance curves are vertically shifted for clarity.

used, contrary to the VSM technique. Additionally, the line width includes information about the absorption and inhomogeneity in the sample. Figure 3 shows the FMR spectra of the samples for different NiFe layer thicknesses for the in-plane geometry with the external field parallel (0) and antiparallel (π) to the exchange anisotropy direction. The observed resonance modes arise from the NiFe layers. The 1.4 nm thick NiFe layer does not give a resonance signal. Similarly, no resonance mode was observed for the CoFe layer in any of the samples. The XRR results indicate that the thickness of the CoFe layers ranges from 1.65 nm to 1.75 nm (see Table 1). As can be seen in Fig. 3, a low thickness accompanied by a high interface roughness causes line broadening in the FMR spectra of the 3.36 nm thick NiFe layer. Accordingly, the non-existent resonance modes of the NiFe (1.4 nm) and CoFe (1.65~1.75 nm) layers can be attributed to their low layer thicknesses and high roughness at the NiFe/IrMn and IrMn/CoFe) interfaces (see Table 1). These results clearly show that ferromagnetic NiFe and CoFe layers with thicknesses below 2 nm and high interface roughness cannot be saturated by the EPR spectrometer at X-band frequencies (9.5-9.8 GHz) at room temperature. Nevertheless, the measured resonance modes shown in Fig. 3 and the results of the XRR study (Table 1) allow a clear discussion on the correlation between exchange bias and the roughness at the NiFe/IrMn interface.

With the in-plane geometry of the applied field, when the external field (H_r) is applied along the direction of H_{ex}, the effective field in each NiFe layer varies from $H_r(0) + H_{ex}$, when H_r and H_{ex} have the same direction, to $H_r(\pi) - H_{ex}$, when they have opposite directions. The difference $[H_r(\pi) - H_r(0)] = 2H_{ex}$ therefore gives the FMR measure of H_{ex} [19, 20]. In Fig. 4, the H_{ex} values (filled triangles in Fig. 4) and the line widths of the FMR spectra, in both parallel and antiparallel directions (open and filled squares), are shown as a function of the inverse NiFe thickness ($1/t_{NiFe}$). H_{ex} decreases with increasing NiFe thickness and indicates the well-known $1/t_{NiFe}$ linear dependence. In addition, the FMR resonance line widths alter with rising NiFe film thickness and indicate almost the same linear variation with $1/t_{NiFe}$ (see Fig. 4). This linear correlation between the line width and the $1/t_{NiFe}$ values has also been reported in NiFe/FeMn based EB systems [21] and is attributed to the interfacial nature of the exchange coupling; however, any correlation with the interface structure (i.e. interface roughness) has not been investigated. In addition to the H_{ex} values, the unidirectional anisotropy energy constant (J_k) was calculated, $J_k = M_s t_F H_{ex}$, where t_F and M_s are the F layer thickness and saturation magnetization, respectively. M_s values were determined from the NiFe thickness dependence of the effective magnetization ($4\pi M_{eff}$) according to the Formula

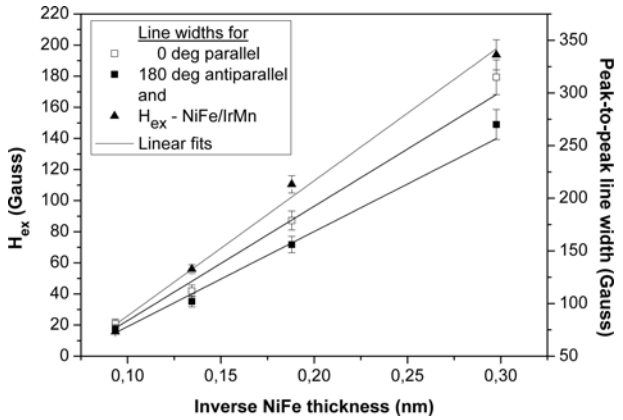

Fig. 4. H_{ex} versus inverse NiFe thickness ($1/t_{NiFe}$, filled triangular) and the evolution of the peak-to-peak line widths of the FMR spectra for the external field parallel (0 deg., open squares) and antiparallel (180 deg., filled squares) to the exchange anisotropy directions. All straight lines are linear fits.

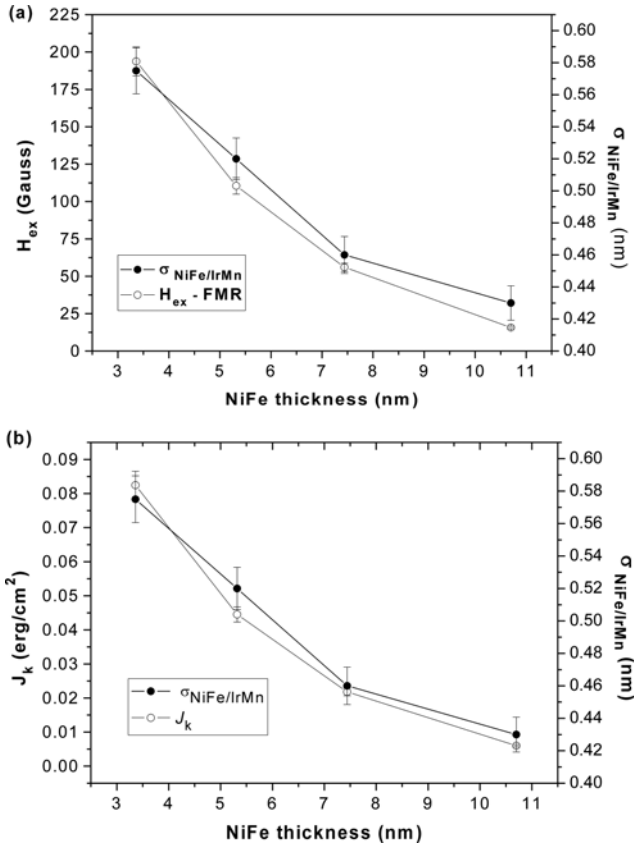

Fig. 5. (a) H_{ex} and (b) J_k (open circles) and the roughness values at the NiFe/IrMn interface (filled circles) and their dependence on the NiFe layer thickness. Lines are guide for the eye.

$M_{eff} = M_s - (2K/M_s t_F)$, where K is the anisotropy constant. The $4\pi M_{eff}$ values were obtained by fitting the out-of-plane angular dependence of the FMR resonance field (details are given in the following part). Figure 5(a), (b) shows the evolution of H_{ex}, J_k and the roughness at the NiFe/IrMn interface and their dependence on the NiFe layer thickness. The H_{ex}, J_k and interface roughness values decrease with increasing NiFe layer thickness and indicate almost the same tendencies. In other words, the H_{ex} and J_k values increase with increasing roughness of the interface. This result reveals the existence of a clear correlation between the H_{ex}, J_k and roughness at the NiFe/IrMn interface in the investigated samples and the importance of the interface structure.

Additional information can be gained by the out of plane angular dependent FMR measurements. The external magnetic field can be continuously rotated in the y/z out of plane direction given by the angle θ_H with respect to z-axis. In the investigated samples, for all angles θ_H of the external magnetic field, only one resonance signal was observed to arise from the NiFe layer (see Fig. 6). This result is in agreement with the results of the in-plane resonance measurements and indicates that the NiFe layer possesses an in-plane easy axis of magnetization. The resonance field (H_R) and the effective magnetization ($4\pi M_{eff}$) can be obtained by fitting the out-of-plane angular dependence of the H_R, specifically we using the well-known relationship given below:

$$(\omega/\gamma)^2 = [H_R \cos(\theta_H - \theta) - 4\pi M_{eff} \cos 2\theta] \times [H_R \cos(\theta_H - \theta) - 4\pi M_{eff} \cos^2 \theta] \quad (1)$$

Here, ω is the microwave angular frequency and $\gamma = ge/2m$ the gyromagnetic ratio. The measured and calculated curves are shown in Fig. 6. H_R and $4\pi M_{eff}$ values were obtained from theoretical fits to the out of plane angular dependent FMR resonance spectra using eq. (1) (see Fig. 6). The evolution of the H_R and $4\pi M_{eff}$ values are shown in Fig. 7 as a function of the NiFe layer thickness. The H_R enhances rapidly from 3.36 nm up to a NiFe thickness of 5.32 nm and then remains almost constant. This rapid increase of the H_R at low thicknesses can be attributed to changes in the interfacial structure, since the XRR results indicate a significant change in the roughness values at the NiFe/IrMn interface (Table 1 and Fig. 5(a), (b)). In contrast to this, the $4\pi M_{eff}$ values increase with increasing NiFe thickness and reach the well-known value of the bulk NiFe (~9600 G) for a NiFe thickness of 7.44 nm. The $4\pi M_{eff}$ value for the NiFe thickness of 10.70 nm is higher than that of the bulk NiFe. A larger $4\pi M_{eff}$ was also reported in NiFe/FeMn EB systems [20], this was attributed to the fact that the uniaxial anisotropy of the exchange-biased NiFe layer is influenced by the unidirectional anisotropy of the AF FeMn layer and, consequently, the effective magnetization of the F NiFe layer is enhanced. Furthermore, the g-factors were calculated according to $g = (h\nu/\mu_B H_R)$. The variation of the g-factors with the thickness of the NiFe layer, shown in the inset picture of Fig. 7, indicates an opposite variation to the H_R values in Fig. 7. The g-factors in the present study are consistent with other published values [22].

As a general result of the FMR and XRR studies, it can be concluded that the evolution of the H_{ex} and J_k at the NiFe/IrMn interface is predominantly affected by interface roughness induced interfacial effects.

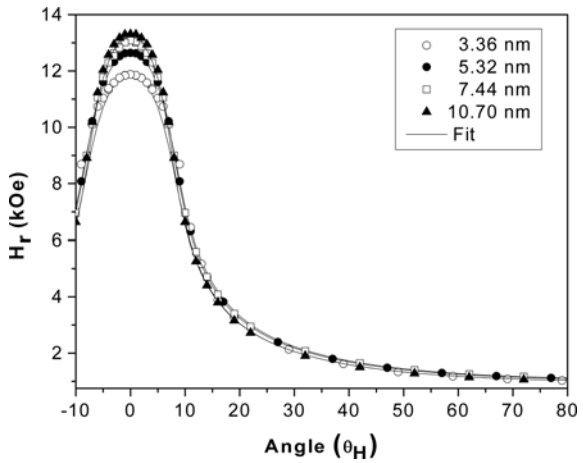

Fig. 6. The out of plane angular dependent FMR resonance spectra for different NiFe thicknesses. All lines are theoretical fits according to eq. (1).

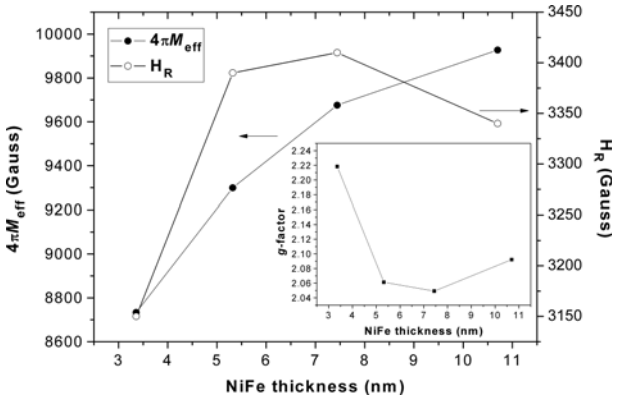

Fig. 7. H_R and $4\pi M_{eff}$ values as a function of the NiFe thickness, which were obtained from the theoretical fits to the out of plane angular dependent FMR resonance spectra using eq. (1) (see Fig. 6). The inset picture shows the variation of the g-factor with NiFe thickness. All lines are guide for the eye.

4. Conclusions

The evolution of the interface roughness and the exchange bias was investigated using X-ray reflectivity and ferromagnetic resonance techniques in the NiFe/IrMn/CoFe system. The X-ray reflectivity measurements reveal that the NiFe layer thicknesses vary between 1.4 nm and 10.7 nm. The FMR results indicate that the ferromagnetic NiFe and CoFe layers with thicknesses below 2 nm and high interface roughness cannot be saturated by the EPR spectrometer at X-band frequencies (9.5~9.8 GHz) at room temperature. Both the exchange bias field and the line widths of the FMR spectra, which were measured for NiFe thicknesses beyond 2 nm, decrease with increasing NiFe layer thickness and indicate the well-known $1/t_{NiFe}$ linear dependence. The exchange bias field, the anisotropy energy constant and the roughness at the NiFe/IrMn interface indicate almost the same NiFe layer thickness dependence, which reveals the influence of the interfacial structure. The influence of the interface roughness is also supported by the out of plane angular dependent resonance measurements, which indicate the interfacial nature of the exchange coupling between NiFe/IrMn layers. By considering the NiFe layer thickness induced variation of the exchange bias field, the anisotropy energy constant and the roughness at the NiFe/IrMn interface, it can be concluded that the exchange bias is significantly affected by NiFe/IrMn interface roughness induced interfacial effects in the investigated samples deposited using the pulsed DC magnetron sputtering technique.

Acknowledgements

This work was partially supported by TUBITAK under Grant. No. MAG-106M517, the Directorate for Scientific Research Projects of Anadolu University under Grant No BAP-050255, the DPT (State Planning Organization of Turkey) through Project No: 2009k120130 and TÜBİTAK-RFBR through Project No: 209T061.

References

[1] W. H. Meiklejohn and C. P. Bean, Phys. Rev. **102**, 1413 (1956).
[2] J. Nogues and K. Ivan Schuller, J. Magn. Magn. Mater. **192**, 203 (1999).
[3] Susumu Soeya, Appl. Phys. Lett. **94**, 242507 (2009).
[4] S. K. Mishra, F. Radu, S. Valencia, D. Schmitz, E. Schierle, H. A. Dürr, and W. Eberhardt, Phys. Rev. B. **81**, 212404 (2010).
[5] K. O. Grady, L. E. Fernandez-Outon, and G. Vallejo-Fernandez, J. Magn. Magn. Mater. **322**, 883 (2010).
[6] R. M. Oksuzoglu, M. Yıldırım, H. Çınar, E. Hildebrandt, and L. Alff, J. Magn. Magn. Mater. **323**, 1827 (2011).
[7] A. M. Zhang, H. L. Cai, and X. S. Wu, J. Supercond. Nov. Magn. **23**, 863 (2010).
[8] V. P. Nascimento, E. C. Passamani, A. D. Alvarenga, F. Pelegrini, A. Biondo, and E. Baggio Saitovitch, J. Magn. Magn. Mater. **320**, e272 (2008).
[9] C. Fleischmann, F. Almeida, J. Demeter, K. Paredis, A. Teichert, R. Steitz, S. Brems, B. Opperdoes, C. Van Haesendonck, A. Vantomme, and K. Temst, J. Apply. Phys. **107**, 113907 (2010).
[10] M. Pakala, Y. Huai, G. Anderson, and L. Miloslavsky, J. Appl. Phys. **87**, 6653 (2000).
[11] Luc Thomas, Béatrice Negulescu, Yves Dumont, Michel Tessier, Niels Keller, André Wack, and Marcel Guyot, J. Appl. Phys. **93**, 6838 (2003).
[12] Congxiao Liu, Chengtao Yu, Huaming Jiang, Liyong Shen, Alexander C, and G. J. Mankey, J. Appl. Phys. **87**, 6644 (2000).
[13] J. Lindner and K. Baberschke, J. Phys.: Condens. Matter **15**, R193 (2003).
[14] B. Aktaş and M. Özdemir, Physica B **125**, 193 (1994).
[15] W. J. Fan, X. P. Qiu, Z. Shi, S. M. Zhou, and Z. H. Cheng, Thin Solid Films **518**, 2175 (2010).
[16] E. Chason and T. M. Mayer, Crit. Rev. Solid State Mater. Sci. **22**, 1 (1997).
[17] O. Baake, R. M. Oksuzoglu, S. Flege, P. S. Hoffmann, S. Gottschalk, H. Fuess, and H. M. Ortner, Materials Characterization **57**, 12 (2006).
[18] R. Mustafa Oksuzoglu, Ian MacLaren, Christoph Schug, and Hartmut Fuess, J. Phys.: Condens. Matter. **17**, 4073 (2005).
[19] W. Stoecklein, S. S. P. Parkin, and J. C. Scott, Phys. Rev. B. **38**, 6847 (1988).
[20] S. J. Yuan, Y. X. Sui, and S. M. Zhou, Eur. Phys. J. B. **44**, 557 (2005).
[21] V. S. Speriosu, S. S. P. Parkin, and C. H. Wilts, IEEE Trans. Magn. **23**, 2999 (1987).
[22] J. P. Nibarger, R. Lopusnik, Z. Celinski, and T. J. Silva, Appl. Phys. Lett. **83**, 93 (2003).